Journal Pre-proof

Impedance spectroscopy for multi-state analysis of dissolvable powders: Determining layer thickness and moisture content

Maximilian Becker, Maike Orth, Anupam Kumar, Dennis Kähler, Matthias Kuhl, Stefan Heinrich, Thorsten A. Kern

PII: S0032-5910(26)00382-7
DOI: https://doi.org/10.1016/j.powtec.2026.122493
Reference: PTEC 122493

To appear in: *Powder Technology*

Received date : 28 November 2025
Revised date : 25 March 2026
Accepted date : 26 March 2026

Please cite this article as: M. Becker, M. Orth, A. Kumar et al., Impedance spectroscopy for multi-state analysis of dissolvable powders: Determining layer thickness and moisture content, *Powder Technology* (2026), doi: https://doi.org/10.1016/j.powtec.2026.122493.

Updated manuscript with highlighted changes

Graphical Abstract

Impedance Spectroscopy for Multi-State Analysis of Dissolvable Powders: Determining Layer Thickness and Moisture Content

Maximilian Becker, Maike Orth, Anupam Kumar, Dennis Kähler, Matthias Kuhl, Stefan Heinrich, Thorsten A. Kern

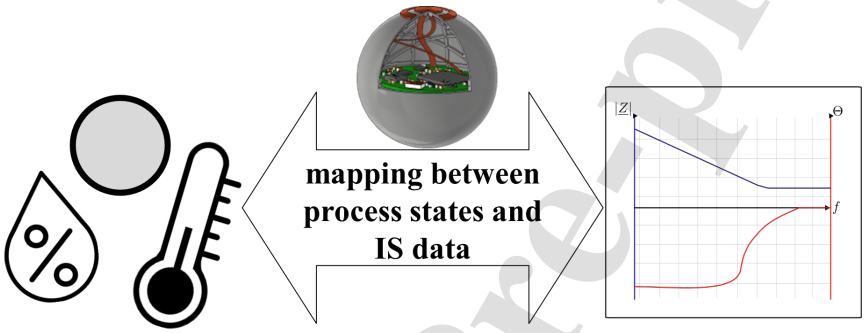

Impedance Spectroscopy for Multi-State Analysis of Dissolvable Powders: Determining Layer Thickness and Moisture Content

Maximilian Becker[a], Maike Orth[b], Anupam Kumar[c], Dennis Kähler[a], Matthias Kuhl[c], Stefan Heinrich[b], Thorsten A. Kern[a]

[a]*Institute for Mechatronics in Mechanics, Hamburg University of Technology, Eissendorfer Str. 38, Hamburg, 21073, Germany*
[b]*Institute of Solids Process Engineering and Particle Technology, Hamburg University of Technology, Denickestraße 15, Hamburg, 21073, Germany*
[c]*Department of Microsystems Engineering, University of Freiburg, Georges-Koehler-Allee 201, Freiburg, 79110, Germany*

Abstract

This study presents a novel methodology for applying Electrical Impedance Spectroscopy to analyze the electrical properties of dissolvable powders, when applied as a coating layer to quantify their thickness and moisture content. To address challenges posed by undefined geometries, powders were dissolved and applied as coatings on custom-designed Printed Circuit Board electrodes. Using sodium benzoate as a model material, the drying process was monitored in off-line measurements, revealing distinct transitions in electrical properties. Impedance and phase angle measurements effectively tracked moisture reduction during drying, while coating thickness and solution concentration also influenced conductivity. The findings demonstrate the potential of this approach for industrial applications, such as fluidized bed spray granulation, by enabling real-time monitoring of drying states.

Keywords: Electrical Impedance Spectroscopy, Fluidized bed coating, SMART particle

1. Introduction

Electrical Impedance Spectroscopy (IS) has emerged as a powerful analytical technique for probing the electrical properties of substrate compositions. By measuring a substrate's impedance across a range of frequencies, IS

provides insight into the substrate's structural and compositional characteristics, allowing for precise detection of changes in and identification of substrate states [1]. Common applications of IS include monitoring corrosion processes in metals (e.g.[2, 3]), evaluating battery performance in energy storage systems (e.g.[4, 5]), and assessing biomaterial properties in biomedical implants (e.g.[6, 7]). In each of these applications, the continuous contact interface between the substrate and the IS system enables reproducible measurements by ensuring stable electrode-substrate connections. For liquid substrates, electrodes can be immersed directly in the medium, achieving high measurement accuracy, whereas solid substrates often allow reliable data collection through firm electrode-to-surface contact [8].

1.1. Applying IS to geometrically undefined interfaces

The beneficial contact interface is compromised when measuring undefined geometries, such as powders, where the measurement outcome depends on various properties including particle density, size, and shape. These factors affect the electrical interface and can lead to significant variability in the impedance response of multiple samples within the same batch. Examples for dissolvable powders are salts that provide high conductivity when dissolved as ionic solution and low conductivity when dry. While IS has been applied to study the effects of the presence of different salts on other materials (such as in corrosion studies on metal surfaces coated with salt layers [9]), it is rarely used to examine the electrical characteristics of the salts themselves. Such measurements of powders pose unique challenges, as the dispersed, heterogeneous structure of the individual particles limits the formation of a uniform conductive path between the electrodes.

1.2. IS in fluidized bed reactors

One apparatus, in which particle systems with distributed properties are processed, is a fluidized bed. Common fluidized bed processes include granulation or coating, during which a solid-containing liquid is sprayed onto fluidized particles and subsequently dried, forming a solid shell [10]. To achieve a high uniform product quality, coating properties, such as moisture and layer thickness, need to be controlled precisely. Various materials can be applied as coating, including crystalline materials like salts such as sodium benzoate. By directly measuring the electrical properties of salt coating layers within the fluidized bed reactor, IS could enable real-time tracking of

parameters that can be correlated to the electrical signal to support optimizing coating uniformity and process efficiency. This real-time monitoring provides critical feedback for controlling the coating process, leading to improved quality and consistency in granule production. Currently, no real-time sensor systems exist for analyzing coating layer formation directly inside fluidized beds. Within a broader research project aimed at developing an instrumented sensor particle that can be inserted into the fluidized bed, the present study focuses on establishing the underlying measurement principle required for such a device. Rather than implementing real-time sensing, this work aims to provide a proof of concept by examining the electrical response of coating layers in a controlled environment. These insights are essential for evaluating the feasibility, operating range, and future design parameters for a particle-based sensor. The scalable measurement approach demonstrated here is intended to support its later integration into a particle-shaped sensing platform suitable for in-line monitoring.

1.3. Outline of this study

To address the above mentioned challenges, this study introduces a novel approach for applying IS to analyze dissolvable powders, as the undefined geometries make this substrate difficult for traditional IS methods. In this method, the powders are first dissolved in deionized water and then applied as a coating onto custom-designed electrodes on Printed Circuit Boards (PCBs) through a controlled drying process to mimic the solid-liquid interaction in a fluidized bed spray coating process. This approach allows for precise monitoring of the electrical properties of the resulting powder layer as it forms and dries, enabling tracking of state changes during the drying process. By focusing on this dynamic process, the methodology provides insights into the electrical behavior of the powder layer under varying moisture levels, supporting applications where understanding the formation and stability of powder coatings is crucial. The use of PCBs with electrodes offers a cost-effective and scalable solution for IS measurements, as highlighted by Goh et al. [11], who reviewed advances in printed electrode technologies for electrochemical applications.

2. Materials and Methods

This section details the materials, measurement setup, and experimental procedures used to implement the proposed Electrical Impedance Spec-

troscopy (IS) methodology for measuring dissolvable powders. In the following, the topics of PCB electrodes, sodium benzoate as a coating material, IS parameters and PCB coating procedures are explained.

2.1. Printed Circuit Board Electrodes

The PCBs are designed to be of two layers with two electrodes on the same side. Figure 1a shows several electrode geometries that were compared to determine the design with the lowest idle impedance. Minimizing idle impedance is a crucial set screw for the Signal-to-Noise Ratio (SNR) of the coating layer impedance, as the specific electrode geometry dictates the setup's capacity and therefore its part of the measurement impedance. This allows for more precise and reliable measurements of the electrical properties of the coating. Each design allows a two-terminal measurement setup, where excitation electrodes are also used as measurement electrodes for both voltage and current. This design includes the contact impedance between electrode and substrate in the measurement, which is treated as additional information in the IS to enable a more detailed post-process interpretation of influencing parameters. The gap between the electrodes is 1 mm for the bigger geometries $V1$ and 0.5 mm for the smaller geometries $V2$ for all geometry layouts, with varying electrode surface areas. The geometric design with the lowest idle impedance was determined through a preliminary study, where the circular electrode design proved to be superior as shown in Figure 1b and even more visible in the according magnification at 100 kHz shown in Figure 1c. While only connected through air in this measurement scenario, causing capacitive impedance results, the electrodes are designed to also connect to materials in a conductive manner. Measurements were conducted with both the conductive as well as the capacitive electrodes in scenarios where reference data was required. The PCBs were ordered from AISLER B.V., NL. The boards have a thickness of 1.6 mm, the base material is *FR4 TG 140 °C* and the electrodes are made of 35 µm copper coated with an *ENIG* finish. The latter stands for a protective layer of nickel and gold [12, 13].

2.2. Electrical Impedance Spectroscopy (IS)

IS was performed using the *MFIA 5 MHz Impedance Analyzer* in combination with the *MFITF Impedance Test Fixture* by Zurich Instruments AG 2024, CH. The device provides a software interface with a frequency sweep tool. Comparability across the measurements was achieved through identical sweep parameters, where the frequency range was set to 1 kHz...1 MHz

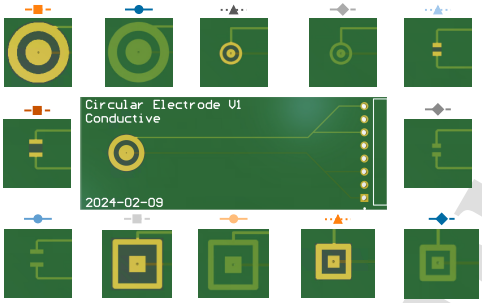

(a) Golden electrodes are made with an ENIG-finish, pale electrodes are covered by the manufacturer's insulating solder mask. Each geometry has a big layout(*V1*) and a small layout (*V2*).

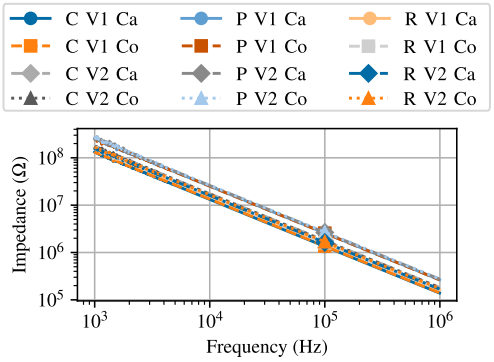

(b) Impedance spectroscopy. Legend in Figure 1a.

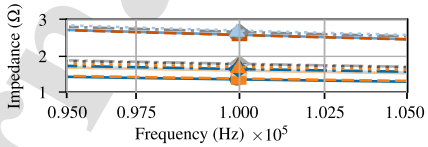

(c) Impedance spectroscopy magnification on 100 kHz. Legend in Figure 1a.

Figure 1: Preliminary electrode comparison of different two-terminal measurement constellations with varying geometries (rectangular, circular, plated) and with/without solder mask (capacitive/conductive) to the determine electrical idle impedance.

with 500 measurement points. The frequency range was chosen to reduce low frequency behavior such as capacitive double layer effects. The voltage

and current limits were set to auto mode to prevent clipping of the signal. This resulted in an excitation signal of up to 3 V and 10 mA [14].

2.3. Sodium benzoate

Sodium benzoate was chosen as exemplary coating material for the experiments in this study. The white, crystalline material is produced by neutralizing benzoic acid with sodium hydroxide and commonly used as a preservative in food and beverages [15].

2.4. PCB experiments

The goals of this study were to identify conductivity changes of the coating during a drying process as well as to establish a mapping of this change to actual process parameters such as layer thickness and moisture content. For this, different measurements were conducted, with the key scenario representing a complete drying process from a solution state to a dried layer of sodium benzoate. The distinct states (liquid, solid coating layer with moisture and dry coating layer) of the coating material during drying are declared as *drying states*. To further investigate those drying states, individual scenarios were introduced to cover measurements of isolated drying states. These scenarios include measurements of solutions with different sodium benzoate concentrations and analysis of the coating layer with respect to its height.

2.4.1. Coating procedure

For coating the PCB surface analogously to a fluidized bed process, a solution of deionized water with 30 wt−% of sodium benzoate was used. Due to poor wetting in a static setting, as discussed in section 3.1, additional spreading with a pipette was necessary to ensure the formation of a thin, uniform film. Comparable drying conditions to an exemplary fluidized bed coating process are achieved through drying in an oven at 80 °C after application of the solution. The temperature was chosen based on preliminary experiments, in which this setting was found to favor the formation of smooth, uniform coating layers.

2.4.2. Continuous drying process

A continuous drying process was emulated in an oven at 80 °C and continuously validated. The sample was measured in an interval of 2 min using IS. To track the moisture content in the sodium benzoate coating, the mass of the coating was measured at each measurement step. For each measurement

step, the sample was taken out of the oven to perform the measurements. Figure 2 illustrates the process.

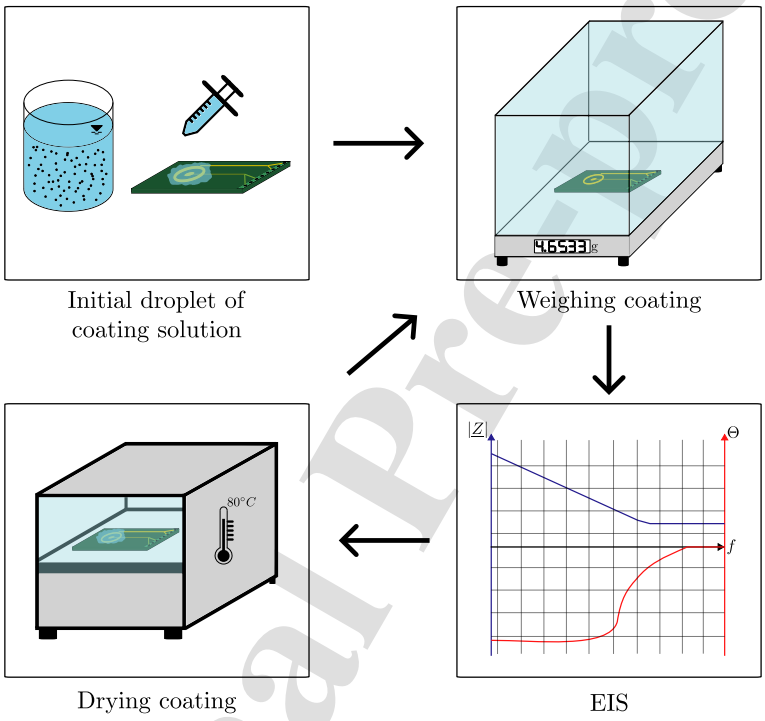

Figure 2: Measurement procedure for a continuous drying process.

2.4.3. Sodium benzoate concentration

During the drying process, water evaporates from the solution leading to an increase in sodium benzoate concentration until it eventually forms a dried coating layer. To determine the transition from the solution to the solid state during drying, it is essential to first correlate the IS data to the sodium benzoate concentration. For this purpose, solutions with varying concentrations of sodium benzoate were analyzed using IS in a separate experiment.

The experimental setup involved circular electrodes of geometry *V1* from Figure 1a, which were immersed in the various solutions. These solutions were contained in beakers and ranged concentration levels from 0 wt−% to 30 wt−% in increments of 5 wt−%.

2.4.4. Coating layer analysis

In the final step of the drying process, a solid layer of sodium benzoate is formed on the electrode. This coating is characterized by its thickness and moisture content. From an electrical point of view, the transition from a solution state to a dried layer is supposed to be a continuous process. By this definition, a completely dried state has to be achieved to derive an isolated correlation between layer thickness and impedance, where the influence of moisture is non-existent. Considering the ability of sodium benzoate to absorb water out of the ambient air, this process was realized by cooling down the coated electrodes in a desiccator after a sufficiently long drying time in the oven. On the one hand, different sodium benzoate coating layer thicknesses were achieved by varying the amount of solution applied to the PCB, on the other hand, additional layers were added after the previous layer was completely dried. To analyze the effect of ambient moisture being absorbed by the sodium benzoate, some samples of dried coating layers were left to cool down without using a desiccator leading to a change in the IS . However, the amount of water absorbed from the ambient air was not detectable when weighing the sample.

2.5. Coating layer thickness

To measure the thickness of the applied sodium benzoate layers, the coated PCBs were analyzed using the *3D Optical Profilometer VR-6000* by Keyence Corporation, JP. A structured light is projected diagonally on the sample by two LEDs. Height differences on the sample surface cause a distortion of the striped light, which is recorded by a camera placed above the stage. From the distorted light projection, the sample height is measured and the three-dimensional surface is reconstructed. Figure 3 shows an exemplary image of a coated PCB as recorded by the profilometer.

As the profilometer is only capable of measuring relative distances, the uncoated PCB surface (area made of *FR4 TG 140 °C*) was defined as reference plane for layer thickness evaluation. This was done to equalize tilted positions of the PCBs and referring the top of the coating layer to the coated surface. Afterwards, a threshold was applied to differentiate between sodium

benzoate coating layer and smaller peaks on the reference plane, such as the remaining copper and the labels. The exact value of the threshold depended on the height of the coating layer and the directly surrounding parts of the PCB for each individual measurement. According to this criterion, the coated area was identified and the average height of the coating above the reference plane was determined.

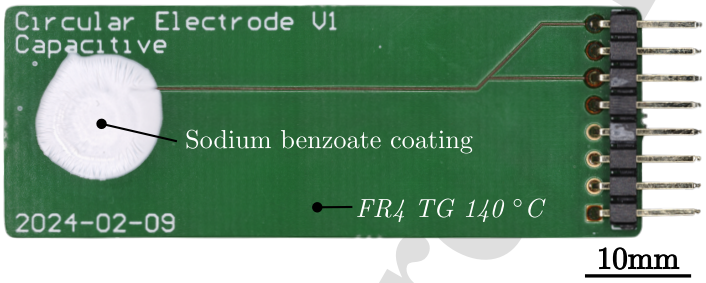

Figure 3: Exemplary coating of a PCB with sodium benzoate.

2.6. Surface characterization

In order to ensure sufficient wettability of the PCBs to achieve an sodium benzoate adequate coating, the roughness of the PCB surface and contact angle of sodium benzoate solution droplets on different materials of the PCBs were analyzed. The former was measured using the same profilometer as for the layer thickness measurements in section 2.5. Measurements were carried out on the capacitive and the conductive electrodes (electrodes with and without soldermask, respectively) as well as on the surrounding base material [12]. Again, the tilted position of the PCBs was corrected to enable evaluation on a horizontal plane. Afterwards, the surface roughness, characterized by the arithmetic mean height, was determined in a circular or rectangular area.

For contact angle measurements according to the sessile drop method, the *goniometer model 100-00-15* by RAMÉ-HART INSTRUMENT CO., USA was used [16]. Images were recorded with a framerate of 1 fps over a duration of 10 min using a video camera (*XC-77CE*, SONY, JP). For each tested surface (ENIG-finish, solder mask, and *FR4 TG 140 °C*) three 10 µL-droplets of an aqueous solution containing 30 wt−% sodium benzoate were analyzed. To determine the contact angle, the circle method was applied using the drop shape analysis program *DSA4* by KRÜSS, GER [17].

3. Results and Discussion

First, the surface characterization of the investigated PCBs is presented with regard to the impact on the coating. Afterwards, different experiments to correlate the IS measurement results to coating layer properties are discussed.

3.1. Contact angle

For all three surfaces (ENIG-finish, solder mask, *FR4 TG 140 °C*) investigated, a decline in contact angle was observed over time, as shown in Figure 4. A constant contact angle was not reached within the measurement time, showing that in a static setting, droplet spreading happens comparatively slow. In a fluidized bed however, spreading is additionally influenced by particle and droplet dynamics.

Similar values were measured on the solder mask of the capacitive electrode, for which the contact angle decreases from $(59.8 \pm 3.2)°$ to $(47.2 \pm 6.6)°$, and on the *FR4 TG 140 °C* surface, where the initial contact angle of $(55.1 \pm 1.4)°$ reaches a value of $(46.9 \pm 1.7)°$ after 10 min. Both curves display a nearly linear behavior. Due to the roughness of 3.81 µm on the capacitive electrode and 2.04 µm on the *FR4 TG 140 °C* surface and the fact, that macroscopic angles were all below 90°, the microscopic contact angle is assumed to be higher than the macroscopic ones [18, 19].

In contrast, the ENIG-finish of conductive electrodes showed a distinct hydrophobicity with a starting angle of $(84.9 \pm 6.2)°$ that initially declines rapidly, before eventually also linearly decreasing to $(67.1 \pm 6.6)°$. Again, as the measured contact angles are below 90°, the microscopic angle is assumed to be lower compared to the measured contact angle due to the surface roughness. However, since the roughness was determined to be 0.94 µm, the contact angle is less influenced compared to the other two surfaces.

With regard to sodium benzoate coating of the PCBs, particularly both conductive and capacitive electrodes, the contact angle measurements indicate, that natural spreading of the droplets might not be sufficient for efficient coverage. Consequently, other experimental methods of this study were adapted to incorporate additional spreading of the liquid with a pipette in order to ensure a full coverage of the electrodes with a thin solution layer. Another approach to improve spreading behavior is the modification of the solid surface by changing the roughness, which has an effect on the macroscopic contact angle [19].

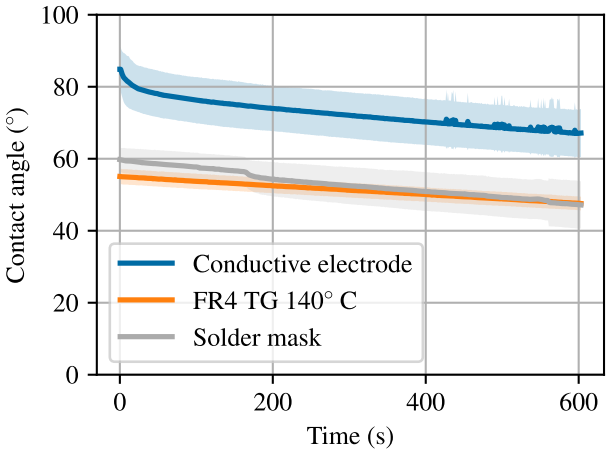

Figure 4: Contact angle of sodium benzoate solution droplets on different PCB surfaces.

3.2. PCB electrodes

First, the results of the PCB measurements during the continuous drying process as described in Section 2.4.2 are discussed. Furthermore, the experiments in Section 3.2.1 and 3.2.2 are used for identification of different drying states within the continuous drying process. The impedance spectroscopy of the continuous drying process is shown in Figure 5 and Figure 6 for conductive and capacitive PCB electrodes, respectively. The measurements were performed using the circular electrode geometry with its bigger geometry shape *V1* as shown in Figure 1a. They include the impedance and phase angle of multiple measurements at different time steps during the drying process from a solution state (high moisture content) to a dried coating layer (low moisture content). Both the conductive and capacitive electrodes show similarities in their change of absolute impedance during drying. This is assumed to be caused by evaporation of water and subsequent solidification of sodium benzoate, which reduce the number of free ions in the moist coating layer, thereby decreasing conductivity and increasing impedance.

Figure 7a shows an impedance range for the conductive electrodes from below 100 Ω to over 100 MΩ throughout the drying process. With decreasing moisture content over the course of drying, higher impedance values are measured, as indicated by the curves moving up in the diagram. Addition-

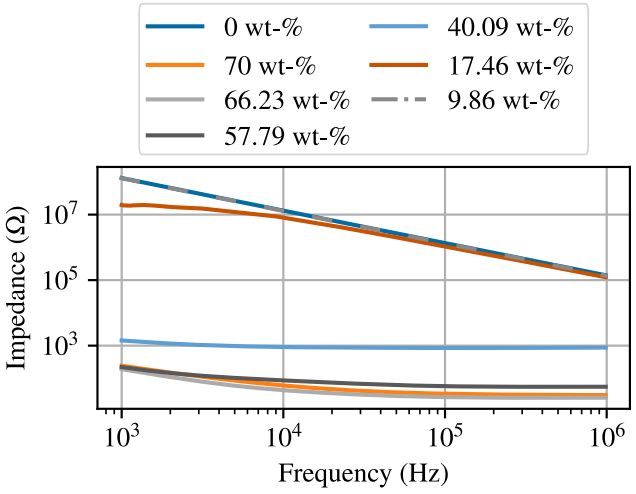

(a) Absolute impedance.

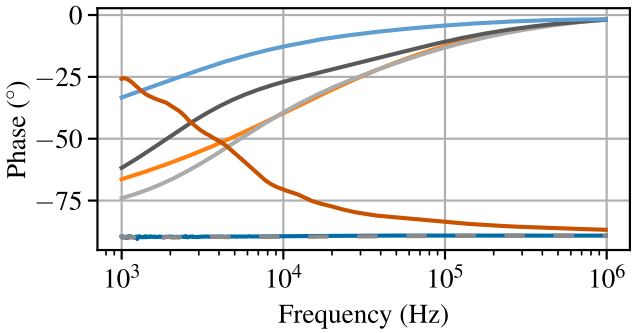

(b) Phase angle.

Figure 5: Impedance spectroscopy throughout the drying process for conductive PCB electrodes with decreasing moisture over the experiment. 0 wt−% corresponds to the uncoated board.

ally, the progress of drying can be observed in the phase angle as shown in Figure 7b, where the shape of the curve changes over moisture. As moisture content decreases, the electrical characteristics transition from a conductive behavior (Phase angle $\approx 0°$), allowing charge to flow, to an insulative behavior (Phase angle $\approx -90°$), where charge is stored. Looking closer at

the difference between uncoated electrodes (0 wt−% water) and electrodes coated with a dried sodium benzoate layer (9.86 wt−% water) shows minimal differences in impedance and phase. This leads to the conclusion that the electrical permittivity ϵ_r of dry sodium benzoate is similar to that of air, making changes to sodium benzoate challenging to detect.

This change directly reflects the drying process, where the loss of the ionic solution causes the sample to lose its ability to conduct current and instead begin to store it. Although the impedance magnitude reflects changes in moisture content, these changes can be inconsistent and abrupt. In contrast, phase angle changes exhibit more stable trends and allow clustering into drying states as can be observed in Figure 7b. When comparing results from Figure 7b with results from measurements in Section 3.2.1 and Section 3.2.2, it is possible to identify a predominantly liquid and a mostly dry state as well as intermediate states of the moist coating layer. Looking at the phase angle in Figure 7b, it slowly approaches the 0° line at 1 kHz for decreasing mositure contents before it completely changes its overall shape at 17.46 wt−%. At the end of the drying process, the phase angle stays almost constantly at −90°. This represents the non-conductive property of dry sodium benzoate and shows its capacitive nature in the setup used. Therefore, Figure 7b supports the ideas of clustering the drying states through the impedance's phase angle while differentiating the drying process within a drying process.

Comparing Figure 6a to Figure 7a shows, that the absolute impedance for capacitive electrodes is generally higher compared to conductive electrodes, although the overall impedance range is narrower. This behavior can be attributed to the default capacitive coupling, which prevents a conductive connection between electrodes, hence causing higher impedances even when measuring a low-resistive solution state. Still, changes in the moisture content of sodium benzoate layers on a capacitive electrode generally had a similar effect on electric behavior in the conductive case: High moisture content resulted in lower impedance values, while dry solid layers had a high impedance, comparable to an uncoated PCB. The shape of the phase angle curve is also affected by the water content, indicating a change in electrical behavior from 10 kHz to 100 kHz. Figure 6b shows that for all moisture levels above 11.64 wt−%, the phase angle changes continuously over the frequency range from 10 kHz to 100 kHz. This change depends on the amount of moisture in the coating layer.

In both cases, conductive and capacitive, the influence of the moisture content can be observed through changes in the complex electrical impedance.

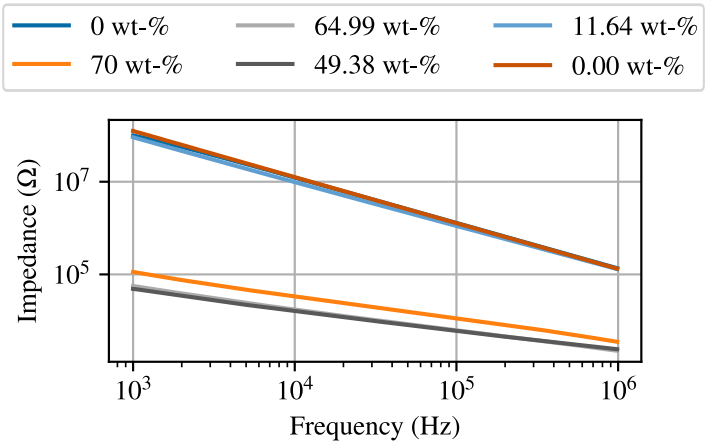

(a) Absolute impedance.

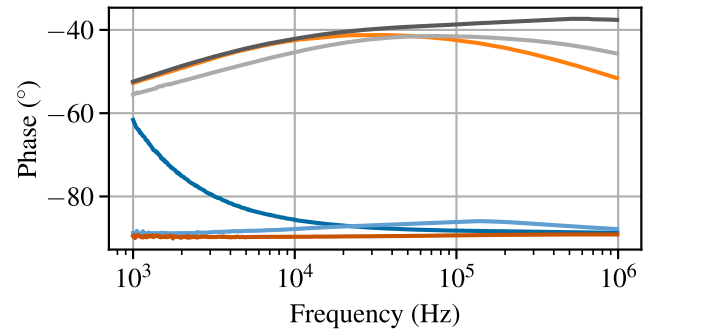

(b) Phase angle.

Figure 6: Impedance spectroscopy throughout the drying process for capacitive PCB electrodes with decreasing moisture over the experiment. 0 wt−% corresponds to the uncoated board.

To showcase this influence in more detail, Figure 7 exemplary shows the impedance and phase angle over moisture content at a frequency of 100 kHz. Interestingly, between 20 wt−% and 40 wt−% water content in the sodium benzoate coating layer, a drastic change in impedance and phase occurs. As described previously, the impedance increases with decreasing moisture content. This may mark the change from a predominantly liquid solution to

a solid layer.

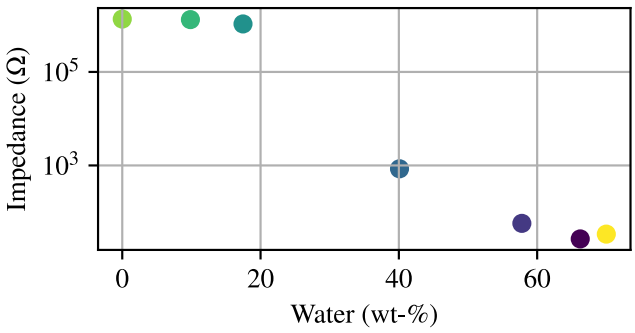

(a) Absolute impedance.

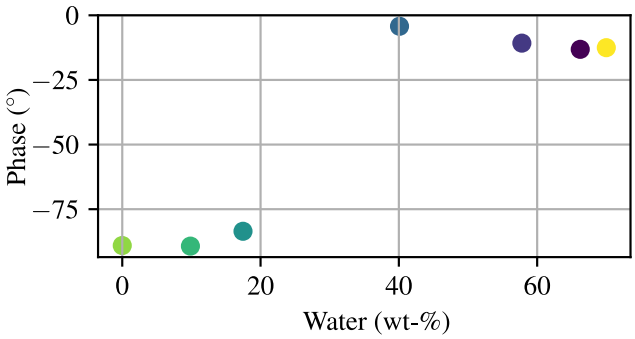

(b) Phase angle.

Figure 7: Impedance of the drying process for conductive electrodes correlating impedance and moisture of the coating layer at 100 kHz. The highest impedance represents the board only (far left) and the highest moisture corresponds to the initial droplet (far right).

Conductive electrodes were chosen for further analysis, as they cover a broader phase angle range than capacitive ones, enabling easier process state discrimination with a single measurement principle.

3.2.1. Sodium benzoate concentration in solution

As the coating process starts with a liquid solution of sodium benzoate and deionized water, influence of sodium benzoate concentration in solution on the impedance was investigated. Figure 8 shows the IS measure-

ment of conductive electrodes in solutions with different concentrations. The impedance plots for different sodium benzoate solution concentrations in Figure 8a reveal the expected increase in conductivity with higher sodium benzoate concentrations due to a higher number of free ions in the solution. Moreover, the impedances measured for all solutions converge from a static decline to a constant absolute value at higher frequencies, as shown in Figure 8a. This behavior reflects the conductive nature of the solution at higher frequencies and the capacitive behavior caused by the double-layer effect at lower frequencies, as described in [1].

A comparison of Figure 8b and Figure 7b reveals that sodium benzoate concentrations during drying can be inferred from matching phase behavior. This can for instance be seen in the shape of the curves of solutions containing $\leq 5\,\mathrm{wt}-\%$ sodium in Figure 8b, which is similar to the phase angle curves of layers with a water content of $57.79\,\mathrm{wt}-\%$ to $70\,\mathrm{wt}-\%$ in Figure 7b.

3.2.2. Coating layer analysis

Throughout the investigation of dried coating layers, an influence of the additional exposure to ambient conditions on the measured impedance became apparent. Due to the hygroscopic nature of sodium benzoate the coating layer can absorb water from the ambient air, which leads to slightly different moisture contents and thus different impedance, when measured directly after drying in an oven or after being exposed to ambient conditions after drying. To keep the moisture content as low as possible but still allow impedance measurement at ambient temperature, coated PCBs were cooled in a desiccator after complete drying. Figure 9 shows the impedance and phase angle of coated PCB directly after drying and after storage in the desiccator for two layer thicknesses. Different thicknesses were achieved by creating an additional coating layer on the electrode, measuring impedance and layer thickness, and afterwards applying more sodium benzoate solution on top of the existing layer and repeating the subsequent steps for layer formation and characterization. The blue curve of the first coating layer was recorded immediately after removal from the drying chamber, once the first coating layer was completely dried. In contrast, the orange curve was measured after a cooling phase in a desiccator. The second layer was measured analogously to the first. While the increased temperature of the electrodes right after the drying process should cause a change in the resistive behavior, the measured phase angles in Figure 9b show a change in the overall characterization represented by a non-constant phase angle over the frequency

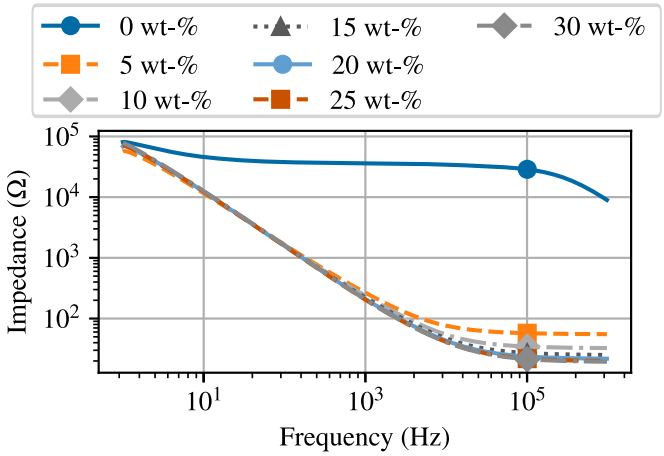

(a) Absolute impedance.

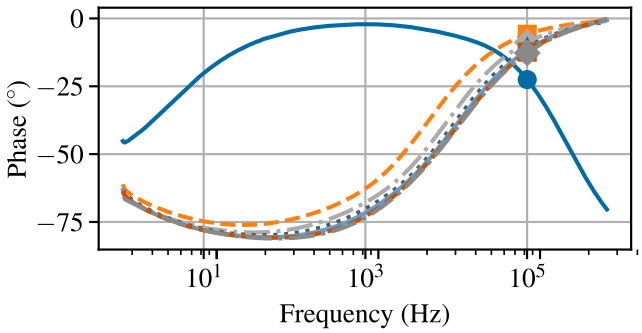

(b) Phase angle.

Figure 8: Impedance spectroscopy of solutions with different sodium benzoate concentrations measured with conductive PCB electrodes.

range. This can be seen especially for the measurement of the second coating layer after the desiccator, where the storage time was significantly longer compared to the first layer. The most likely interpretation for the different measurement results is the absorption of ambient humidity by the hygroscopic sodium benzoate layer even inside the desiccator if the storage time is sufficiently long. In contrast to storage time, the effect of the temperature

was negligible. This is represented by the minor difference in the impedance measured for the first layer right after the drying compared to its measurement after the cool down phase. Because of these observations, subsequent measurements were taken right after taking the samples out of the drying chamber to avoid any absorption of water before the measurement.

Consequently, in a second experimental series, the effect of coating layer thickness was isolated by avoiding the cooling phase and measuring impedance immediately after drying. Figure 10 shows the corresponding results. Here, the phase angle in Figure 10b remains consistently at $-90°$ across all tested frequencies, indicating no or very low moisture in the coating layer. The noise in the lower frequency area likely results from the measurement setup. At high impedances ($\leq$1 MΩ), the measured currents are small, resulting in a low signal-to-noise ratio, where a small amount of noise significantly impacts the results. Due to this, only higher frequencies were taken into consideration. For instance, when magnifying the impedances in Figure 10a at, for example, 100 kHz, a decrease in impedance compared to an uncoated electrode is observed, suggesting a higher relative permittivity. Although differences in layer thickness are visible as differences in the electrical impedance, those differences are small and therefore only visible through magnifications in Figure 10c. This result leads to the conclusion, that IS is less sensitive to the layer thickness compared to the moisture parameter. Nevertheless, Figure 10 shows a clear trend over a wide span of thickness values. Coatings produced in fluidized bed processes are usually thinner than the layers on PCBs measured in this paper [22]. However, the correlation between layer thickness and impedance shown in Figure 10 is assumed to be similar for lower thickness values as long as the electrode is covered. The measurability of these differences allows observation of changes in the coating layer thickness in dried layers via IS .

Final remarks to the measurement principles

The continuous drying experiment is characterized by several execution steps and possible variations that are ideally controlled. These variations include the amount of applied solution, the spreading method, the position in the drying chamber, and the ambient conditions, among other influencing factors. This results in a sensitive procedure with challenging reproducibility even with reproducibility in mind, leading to at least slight variations in measurement data for each repetition. The data presented in this study shows the overall trend observed in all measurements alongside a representative measurement series. Exemplarily, for conductive electrodes covered by a

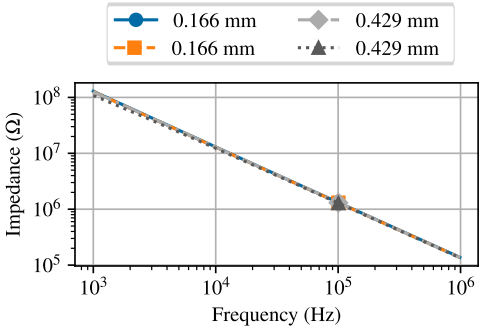

(a) Absolute impedance.

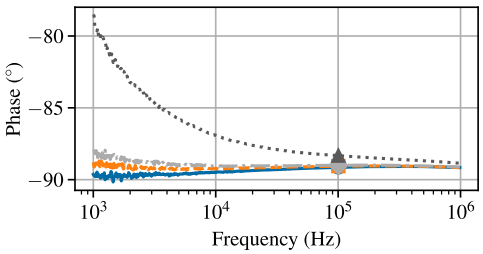

(b) Phase angle.

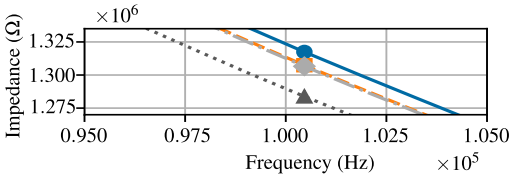

(c) Absolute impedance magnification at 100 kHz.

Figure 9: Impedance spectroscopy of a multilayer coating that experienced absorption of humidity from ambient air. The blue and light gray measurements were taken right after the drying chamber, while the other two measurements were taken after storage in a desiccator.

sodium benzoate coating with a moisture content of approximately 58 wt−%, the impedance spans 211 Ω to 280 Ω at 1 kHz and 53 Ω to 111 Ω at 1 MHz;

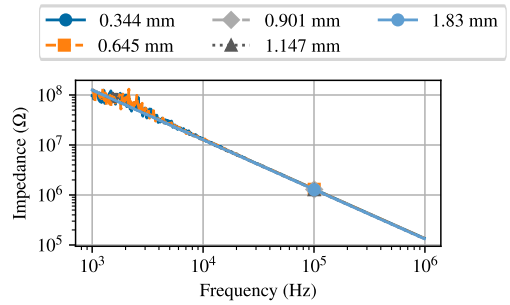

(a) Absolute impedance.

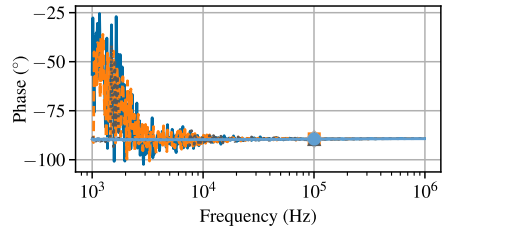

(b) Phase angle.

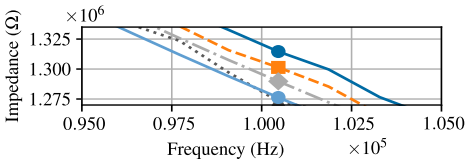

(c) Absolute impedance magnification at 100 kHz.

Figure 10: Impedance spectroscopy of dried sodium benzoate layers of different layer thickness measured with conductive electrodes.

the corresponding phase angles range from −66° to −54° and from −2.1° to −1.9°, respectively.

One challenge was the timing of the drying process, as each IS measurement required approximately 1.5 min, thereby limiting the achievable temporal resolution which is connected to e.g. varying temperatures and continued drying during the IS measurement. Ensuring that the applied solution vol-

ume did not lead to detachment of the coating layer during the falling rate period was also required [20].

Another challenge in forming the coating layer on the electrodes occurs due to the crystalline nature of sodium benzoate. When applied as aqueous solution and subsequently dried, the coating layer structure is influenced by the evaporation rate of the water as crystal formation is affected, as observed by Orth et al.[21]. In order to produce uniform coating layers made of sodium benzoate, as characterized by a smooth surface and mostly constant thickness, that are in contact with the whole electrode, the drying temperature was set to 80 °C as mentioned in Section 2.4.1. At these drying conditions, the solid layer stayed in contact with the electrode while only showing minimal crystal growth and providing an overall smooth layer surface. However, the extent, to which growing of the sodium benzoate crystals occurred, was not completely equal for all experiments.

To evaluate the specific impact of variables like moisture content, temperature and layer thickness, this study isolated each effect in distinct measurement scenarios. While this confirms that IS can successfully detect and trance impedance changes back to these individual origins, translating these signals into validated, absolute measurements of individual properties in an uncontrolled environment, where effects overlap, need to be investigated in future studies. Nevertheless, these isolated scenarios successfully prove the general measurability of layer properties via IS , even with a general electrode-substrate interface.

4. Conclusion

In this study, a novel method was developed for applying Electrical Impedance Spectroscopy (IS) to analyze the electrical properties of salt coating layers, specifically sodium benzoate. Traditional IS approaches encounter substantial difficulties when applied to powders, as undefined geometries and variable substrate–electrode interfaces lead to inconsistent measurements. The method proposed here addresses these limitations by dissolving the salts in deionized water and forming controlled, reproducible coatings on custom-designed Printed Circuit Board (PCB) electrodes through a defined drying process.

The experimental results show that the method can capture characteristic changes in electrical properties during drying, enabling observation of the transition from aqueous solution to solid crystalline material. Under idealized

conditions, systematic dependencies on moisture content and layer thickness were clearly identified, and an impedance range relevant for later in-line monitoring was established. However, the study also reveals several factors that limit measurement reproducibility, including humidity uptake by the salts, temperature- and time-dependent crystallization behavior, and sensitivity to drying dynamics. These influences led to hardly predictable impedance deviations between repeated measurements, highlighting the sensitivity of the method to small variations in environmental and process conditions.

The variability observed indicates that precise, standalone state identification based solely on single-point impedance values may not be feasible without a thoroughly populated data base. Nevertheless, when considering the characteristic evolution of the impedance signal during continuous drying, the method shows promise for tracking transitional states over time, which is particularly relevant for in-process monitoring in coating and spray-granulation operations. Furthermore, the salt used in this study (sodium benzoate) was not tailored for the experiments and highlights the potential of the presented method to be applied to similarly dissolvable substrates which would otherwise be difficult to analyze electrically due to their undefined geometries as powders.

Overall, this study advances the application of Electrical Impedance Spectroscopy to salt-based particle systems and provides a foundational measurement approach that supports the development of continuous, transition-oriented monitoring strategies in industrial coating processes.

Associated Content

Data Availability Statement

The experimental measurement data and electromagnetic simulation models generated and analyzed during this study are openly available in the TUHH Open Research (TORE) repository at `https://doi.org/10.15480/882.16823`.

Acknowledgment

This project is funded by the Deutsche Forschungsgemeinschaft (DFG, German Research Foundation) – SFB 1615 – 503850735.

References

[1] A. C. Lazanas and M. I. Prodromidis, "Electrochemical Impedance Spectroscopy—A Tutorial," *ACS Meas. Sci. Au*, vol. 3, no. 3, pp. 162–193, Jun. 2023. doi: 10.1021/acsmeasuresciau.2c00070.

[2] M. Kaseem, M. P. Kamil, J. H. Kwon, and Y. G. Ko, "Effect of sodium benzoate on corrosion behavior of 6061 Al alloy processed by plasma electrolytic oxidation," *Surface and Coatings Technology*, vol. 283, pp. 268–273, Dec. 2015. doi: 10.1016/j.surfcoat.2015.11.006.

[3] Hoshi, Yoshinao & Soukura, Masanori & Shitanda, Isao & Itagaki, Masayuki & Kato, Yoshitaka. (2015). "Corrosion Monitoring of Reinforcing Steel in Concrete By Electrochemical Impedance Spectroscopy". *ECS Meeting Abstracts*. MA2015-01. 1083-1083. 10.1149/MA2015-01/12/1083.

[4] Q. Zhang, C. -G. Huang, H. Li, G. Feng and W. Peng, "Electrochemical Impedance Spectroscopy Based State-of-Health Estimation for Lithium-Ion Battery Considering Temperature and State-of-Charge Effect" in *IEEE Transactions on Transportation Electrification*, vol. 8, no. 4, pp. 4633-4645, Dec. 2022, doi: 10.1109/TTE.2022.3160021.

[5] M. Messing, T. Shoa, S. Habibi, "Estimating battery state of health using electrochemical impedance spectroscopy and the relaxation effect". *Journal of Energy Storage*, Volume 43, 2021, 103210, ISSN 2352-152X, 10.1016/j.est.2021.103210.

[6] A. Weltin, J. Kieninger, G. A. Urban, S. Buchholz, S. Arndt, and N. Rosskothen-Kuhl, "Standard cochlear implants as electrochemical sensors: Intracochlear oxygen measurements in vivo," *Biosensors and Bioelectronics*, vol. 199, p. 113859, Mar. 2022. doi: 10.1016/j.bios.2021.113859.

[7] D. De Dorigo et al., "A 0.00175 mm^2/channel Direct-Digitization Frontend with Automatic EDO/Drift Compensation for Floating Subcortical Neural Probes," in *2024 IEEE European Solid-State Electronics Research Conference (ESSERC)*, Bruges, Belgium, Sep. 2024, pp. 416–419. doi: 10.1109/ESSERC62670.2024.10719430.

[8] Arduini F, Cinti S, Mazzaracchio V, Scognamiglio V, Amine A, Moscone D. Carbon black as an outstanding and affordable nanomaterial for electrochemical (bio)sensor design. *Biosens Bioelectron.* 2020 May 15;156:112033. doi:10.1016/j.bios.2020.112033. Epub 2020 Jan 29. PMID: 32174547 .

[9] BMin Cao, Li Liu, Zhongfen Yu, Lei Fan, Ying Li, Fuhui Wang. Electrochemical corrosion behavior of 2A02 Al alloy under an accelerated simulation marine atmospheric environment[J]. *J. Mater. Sci. Technol.*, 2019, 35(4): 651-659. 10.1016/j.jmst.2018.09.060

[10] H. Uhlemann and L. Mörl, *Wirbelschicht-Sprühgranulation*. Springer-Verlag, Mar. 2013. ISBN: 978-3-642-57004-9 .

[11] G. L. Goh et al., "Potential of Printed Electrodes for Electrochemical Impedance Spectroscopy (EIS): Toward Membrane Fouling Detection," *Adv. Elect. Materials*, vol. 7, no. 10, p. 2100043, Oct. 2021, doi: 10.1002/aelm.202100043.

[12] AISLER B.V. 2025, "PCB Portfolio - Beautiful Boards / PCB Specification," AISLER Creative Community, Nov. 2024. [Online]. Available: `https://community.aisler.net/t/pcb-portfolio/101`. [Accessed: 27-Feb-2025].

[13] AISLER B.V. 2025, "PCB Surface Finish - AISLER Learning / PCB Design," AISLER Creative Community, Jun. 2024. [Online]. Available: `https://community.aisler.net/t/pcb-surface-finish/4078`. [Accessed: 27-Feb-2025].

[14] Zurich Instruments AG 2025, "MFIA 500 kHz / 5 MHz Impedance Analyzer | Zurich Instruments," Dec. 2019. [Online]. Available: `https://www.zhinst.com/en/products/mfia-impedance-analyzer`. [Accessed: 27-Feb-2025].

[15] E. A. Baldwin, M. O. Nisperos-Carriedo, and R. A. Baker, "Use of edible coatings to preserve quality of lightly (and slightly) processed products," *Crit. Rev. Food Sci. Nutr.*, vol. 35, no. 6, pp. 509–524, Nov. 1995, doi: 10.1080/10408399509527713 .

[16] D. N. Staicopolus, "The computation of surface tension and of contact angle by the sessile-drop method," *J. Colloid Sci.*, vol. 17, no. 5, pp. 439–447, Jun. 1962, doi: 10.1016/0095-8522(62)90055-7 .

[17] KRÜSS Scientific, "Circle method," [Online]. Available: `https://www.kruss-scientific.com/en/know-how/glossary/circle-method`. [Accessed: 27-Feb-2025].

[18] R. N. Wenzel, "Surface Roughness and Contact Angle," *J. Phys. Chem.*, vol. 53, no. 9, pp. 1466–1467, Sep. 1949. doi: 10.1021/j150474a015.

[19] S. Palzer, C. Hiebl, K. Sommer, and H. Lechner, "Einfluss der Rauhigkeit einer Feststoffoberfläche auf den Kontaktwinkel," *Chemie Ingenieur Technik*, vol. 73, no. 8, pp. 1032–1038, 2001. doi: 10.1002/1522-2640(200108)73:8<1032::AID- CITE1032>3.0.CO;2-K.

[20] J. F. Richardson, J. H. Harker, and J. R. Backhurst, "CHAPTER 16 - Drying," in *Chemical Engineering (Fifth Edition)*, Oxford: Butterworth-Heinemann, Jan. 2002, pp. 901–969. doi: 10.1016/B978-0-08-049064-9.50027-8.

[21] M. Orth, P. Kieckhefen, S. Pietsch, and S. Heinrich, "Correlating Granule Surface Structure Morphology and Process Conditions in Fluidized Bed Layering Spray Granulation," *KONA Powder and Particle Journal*, vol. 39, no. 0, pp. 230–239, Jan. 2022. doi: 10.14356/kona.2022016.

[22] S. Pietsch, A. Peter, P. Wahl, J. Khinast, and S. Heinrich, "Measurement of granule layer thickness in a spouted bed coating process via optical coherence tomography," *Powder Technology*, vol. 356, pp. 139–147, Aug. 2019. doi: j.powtec.2019.08.022

- Developed a novel method for coating layer characterization using IS
- Correlated moisture content and coating layer thickness to electrical properties
- Demonstrated potential for monitoring of fluidized bed spray granulation

Declaration of interests

☐ The authors declare that they have no known competing financial interests or personal relationships that could have appeared to influence the work reported in this paper.

☒ The authors declare the following financial interests/personal relationships which may be considered as potential competing interests:

Maximilian Becker reports financial support was provided by German Research Foundation. Maike Orth reports financial support was provided by German Research Foundation. Anupam Kumar reports financial support was provided by German Research Foundation. If there are other authors, they declare that they have no known competing financial interests or personal relationships that could have appeared to influence the work reported in this paper.